ADVANCED ENERGY MATERIALS
www.advenergymat.de

Polysulfonated Fluoro-oxyPBI Membranes for PEMFCs: An Efficient Strategy to Achieve Good Fuel Cell Performances with Low H_3PO_4 Doping Levels

*Davide Carlo Villa, Simone Angioni, Sonia Dal Barco, Piercarlo Mustarelli, and Eliana Quartarone**

Polybenzimidazoles (PBIs) are promising materials to replace Nafion as the electrolyte in polymer electrolyte membrane fuel cells (PEMFCs). The challenge with these materials is to achieve a good compromise between the H_3PO_4 doping level and membrane stability. This can be obtained by a proper monomer design, which can lead to better performing membrane electrode assemblies (MEAs), in terms of durability, acid leaching, and electrode safety. Here the easy and inexpensive synthesis of hexafluoropropylidene oxyPBI (F_6-oxyPBI) and bisulfonated hexafluoropropylidene oxyPBI (F_6-oxyPBI-$2SO_3H$) is reported. The membranes based on F_6-oxyPBI-$2SO_3H$ are more stable in an oxidative environment and more mechanically resistant than standard PBI and F_6-oxyPBI. Whereas the attainable doping levels are low because of fluorine-induced hydrophobicity, polysulfonation allows high proton conductivity, and fuel cell performances better than those reported for MEAs with F_6PBI- or PBI membranes with much higher doping levels. In the case of MEA with a F_6-oxyPBI-$2SO_3H$ membrane, a peak power density of 360 mW cm^{-2} is measured. Fuel cell performances of 604 mV at 0.2 A cm^{-2} are maintained for 800 h without membrane degradation. Low H_2 permeability is measured, which remains almost unaffected during a 1000 h life-test.

1. Introduction

Polymer membranes suitable to be used as electrolytes in polymer electrolyte membrane fuel cells (PEMFCs) for automotive applications should work at least at 120 °C in order to allow efficient heat dissipation,[1] with a proton conductivity, $\sigma \geq 0.1$ S cm^{-1} at relative humidity, *R.H.* < 50%. From this point of view, polybenzimidazole (PBI)-based membranes seem very promising because of excellent thermal stability, and good proton transport properties even under low humidification conditions.[1,2] However, proton conductivity of commercial PBI exceeds 0.1 S cm^{-1} only above 150 °C and at high doping levels, *N*, of phosphoric acid (*N* > 6 mol H_3PO_4, PA, per monomer unit), which reduces their mechanical and thermal stability. Recently, however, several different approaches allowed to reach high conductivity at temperature as low as 120 °C, and namely: i) a proper design of the monomer repeat unit;[2–8] ii) dispersion of functionalized inorganic fillers;[9–11] iii) use of polymer blends;[4] iv) in situ doping procedure of the membrane in order to reach very high dopant content;[4] v) synthesis of block copolymers;[2,4] and vi) crosslinking processes.[4,12]

In this frame, a major technological challenge is to properly balance the PA doping level, which is related to the proton conductivity, with the long-term stability properties of the membrane. Too much PA leads to issues severely limiting cell durability, such as acid leaching of H_3PO_4, cathode poisoning and worsening of the electrolyte mechanical stability. Recently, we showed that polysulfonation is an efficient route to improve the proton transport at low relative humidity, while maintaining a low doping level.[8,13] At 120 °C, for example, conductivity values higher than 10 and 30 mS cm^{-1} were obtained at *R.H.* = 30% and 50%, respectively, for membranes with *N* < 6. Very promising electrochemical performances were also found for membrane electrode assemblies (MEAs) based on these sulfonated systems. In particular, a power density peak of 320 mW cm^{-2} and cell potential of 0.588 V were obtained without membrane degradation over about 200 h at 150 °C.[13]

Due to the rich chemistry of benzimidazole, PBI may be also easily functionalised by introducing fluorine atoms along the polymer backbone. The presence of fluorine atoms confers better organo-solubility to the system due to the flexibility of the $-C(CF_3)_2-$ group, higher chemical stability against oxidation, and also an improved capability as a methanol barrier.[14–19]

Here, we report on the synthesis of a novel fluoro-sulfonated PBI and on its performances in PEMFCs working at temperatures lower than 150°C, low relative humidity (*R.H.* < 50%), and low H_3PO_4 content. We moved through three steps: i) the selection of a monomer unit, containing a higher number of basic nitrogen units with respect to the conventional PBI, in order to improve the acid retention capability of the membrane; ii) the introduction of a fluorinated spacer in order to enhance

D. C. Villa, S. Angioni, S. D. Barco, P. Mustarelli, Prof. E. Quartarone
Department of Chemistry and INSTM
University of Pavia
Via Taramelli 10, 27100, Pavia, Italy
E-mail: eliana.quartarone@unipv.it

DOI: 10.1002/aenm.201301949

the chemical and mechanical stability of the doped membranes; and iii) the polysulfonation of the spacer to increase the proton conductivity even in case of low acid doping level. Two polymers were synthesized by means of microwave assisted organic synthesis (MAOS) technique, and namely hexafluoropropylidene-oxyPBI (F_6-oxyPBI) and sulfonated hexafluoropropylidene-oxyPBI (F_6-oxyPBI-2SO_3H). Membranes doped with different doping levels were obtained by using H_3PO_4 concentrations ranging from 30% to 70%, and fully characterized in terms of chemical, thermal and mechanical stability, proton conductivity and electrochemical tests. The results were compared with those of poly(2,2-(2,6-pyridin)-5,5-bibenzimidazole) (PBI_5N) which, to the best of our knowledge, is one of the most performing modifications of the benzimidazole monomer ever obtained. Our main aim here is to verify if properly designed systems with low amounts of phosphoric acid may likewise provide comparable fuel cell performances and durability with respect to PBI membranes with much higher acid contents, as those generally reported in the literature.

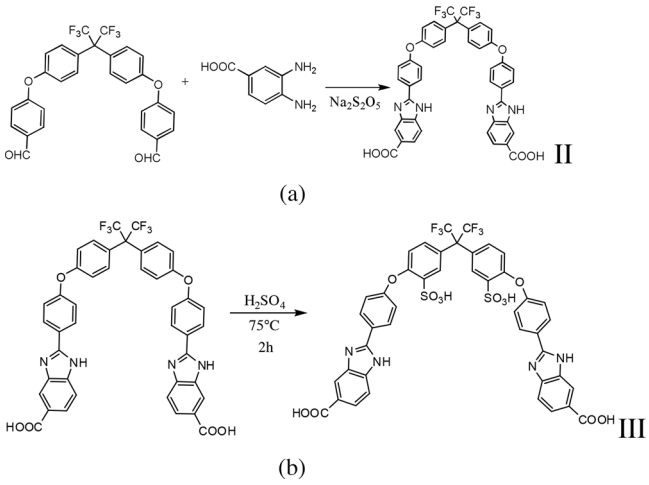

Scheme 2. a) Synthesis of monomer II, F_6-oxyBI; b) Synthesis of monomer III, F_6-oxyBI-2SO_3H.

2. Results and Discussions

2.1. Fluoro-oxy- and Sulfonated Fluoro-oxyPBI

As described in the experimental details, new fluorine-based PBIs were synthesized by means of a polycondensation reaction between diaminobenzidine and monomers II and III, as reported in **Scheme 1**, **2**, **3**. The introduction of fluorine atoms along the polymer backbone aims to improve some properties of PBI such as flexibility, solubility, processability, mechanical and chemical stability. In addition, polysulfonation may contribute to enhance the proton conductivity of membranes with lower doping level, due to a compensation effect provided by additional protogenic groups, such as SO_3H.[13]

The syntheses of F_6-oxyPBI and F_6-oxyPBI-2SO_3H were firstly optimized by characterizing the starting monomers, II and III, and by measuring the inherent viscosity of the resulting polymers. **Table 1** reports some chemical and physical properties of the fluoro-based PBIs, and namely the polymer inherent viscosity, the weight loss in oxidative environment, and the doping levels at different acid concentrations. Table 1 also reports the $[M\text{-}H]^-/z^-$ signals of the mass spectra obtained for each monomer by means of electrospray ionization mass spectrometry (ESI-MS). The experimental molecular weight determined by ESI-MS is in excellent agreement with the nominal ones, so confirming the supposed structure of the monomers, as well as the sulfonation degree in case of F_6-oxyPBI-2SO_3H. The NMR spectra of the monomers (see Experimental Section) also confirm the results obtained by means of mass spectrometry. The 90° pulse ^{13}C DEPT spectra show the correct number of C–H bonds in each monomer, thus indicating the success in controlling polysulfonation for F_6-oxyPBI-2SO_3H. A further confirmation of the monomer structures is provided by ^1H NMR signals, displaying a molecular symmetry in the polysulfonated compound.

In order to prepare mechanically stable and workable membranes, polymers with high molecular weight should be synthesized. In terms of inherent viscosity, *I.V.*, this means to obtain materials with *I.V.* values exceeding 1.0 dL g^{-1}.[2] Table 1 reports the inherent viscosity of both F_6-oxyPBI and F_6-oxyPBI-2SO_3H, namely 1.17 and 0.83 dl g^{-1} respectively, which are in good agreement with data reported in the literature for other fluorinated systems obtained under similar polymerization conditions.[18] In spite of the large monomers dimension, both the polymers were produced with a high molecular weight. In the particular case of the sulfonated one, the relatively good inherent viscosity (0.83 dL g^{-1}) seems to suggest that the polysulfonation step preceding the polymerization does not affect the monomer reactivity. However, F_6-oxyPBI-2SO_3H shows inherent viscosity lower than that of F_6-oxyPBI. A reduced viscosity for sulfonated-PBI with respect to the non-sulfonated ones has been already reported in literature.[13,20] Nevertheless, in both cases homogeneous polymer films with good free-standing properties were obtained. The stiffness of the F-based PBIs was also confirmed by means of mechanical tests. In Table 1 the tensile strengths and the elongations at break of the undoped membranes are reported. Both the dry membranes have a small elongation at break (3–4%), and tensile strength of about 40 MPa at room temperature. Such results

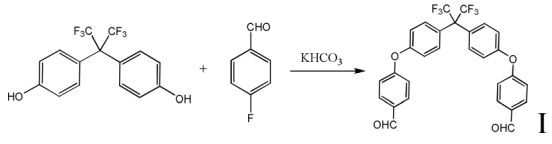

Scheme 1. Synthesis of fluorurated dialdehyde I.

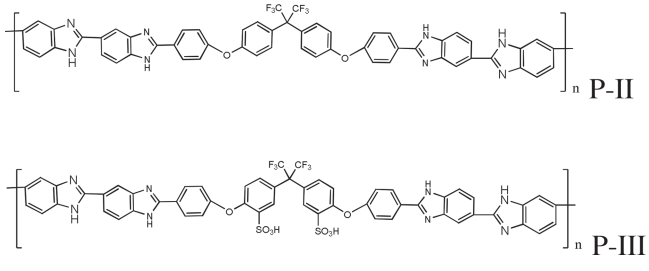

Scheme 3. Structure of F_6-oxyPBI (P-II) and F_6-oxyPBI-2SO_3H (P-III).

Table 1. Nominal and experimental (from ESI-MS measurements) molecular weights of the monomer, polymers weight loss from the Fenton test, polymer inherent viscosity, mechanical properties and doping level for all the investigated polymers.

PBI	MW_{mon} [g mol^{-1}]	ESI-MS [M-H]$^-$/z$^-$	Weight loss [%]	*I.V.* [dl g^{-1}]	Elongation at Break [%]	Stress at Break [MPa]	$DL_{30\%}$ [%]	$DL_{50\%}$ [%]	$DL_{70\%}$ [%]
F_6-oxyPBI	808	807.25	2.0	1.17	3	44.4	26	58	99
F_6-oxyPBI-2SO_3H	968	967.17	5.3	0.83	4	43.0	24	32	77

also demonstrate that the two sulfonic groups do not affect the mechanical properties. These values are in nice agreement with what found by Chuang and co.[14] for linear undoped hexafluoropropylidene-based PBIs (F_6-PBI). However, we stress that a direct comparison of the mechanical properties among different systems is meaningful only in case of similar inherent viscosities and polymer molecular weights.

2.2. Oxidative and Thermal Stability

In order to obtain long-term durability during operation, the membranes should have high chemical resistance in an oxidative environment. An important target to be competitive with the Nafion-based electrolytes consists of very low membrane degradation rate in presence of the peroxide and hydroxyl radicals. The PBI chemical stability was investigated by means of Fenton test, which determines the weight losses of the membranes treated in a 3 wt% H_2O_2 solution containing 4 ppm of $FeSO_4$. Table 1 reports the mass losses of F_6-oxyPBI and F_6-oxyPBI-2SO_3H, detected at 90 °C after a test period of 48 h. We observed that: 1) F_6-oxyPBI exhibits a very low weight loss (≈2%), which is comparable to what observed for Nafion 115 and hexafluoropropylidene-PBI (F_6-PBI), treated in similar conditions and for the same ageing time;[19] 2) In case of polysulfonated fluoro-PBI, a higher mass change is observed (≈5%), which may be likely related to one or two concurrent factors: the presence of the sulfonic groups, as already observed in literature,[13,21] but also the lower polymer molecular weight. Polymers with low *I.V.*s are generally less resistant to the Fenton test; [22] and 3) the introduction of two –CF_3 units in the backbone leads to membranes more chemically stable than those obtained from similar non-fluorinated monomers.[10,13]

The influence of the monomer structure on the polymer thermal stability was investigated by means of Hi-Res Thermogravimetry from room temperature to 900 °C under N_2 atmosphere. The TGA plots of F_6-oxyPBI and F_6-oxyPBI-2SO_3H are reported in the Supporting Information (Figure S1). Both the membranes, as expected, decompose above 450 °C. The non-sulfonated membrane shows a higher degradation onset, which exceeds 500 °C. Such a difference was observed also in case of similar non-fluorinated aryloxy-based PBI and it is related to the degradation of the sulfonic groups.[13] The weight loss of F_6-oxyPBI detected between 400 and 600 °C was about 15%, whereas a higher change is detected for the sulfonated membrane (22%) in the same temperature range. Moreover, the presence of fluorine into the backbone confers a hydrophobic nature to the PBIs. In fact, the weight loss detected below 200 °C, which reasonably is due to the adsorbed water, accounts only for about 2%.

2.3. Doping Level and Mechanical Strength

As stated in the Experimental Section, the acid doping level, *DL*, was measured by titrating the doped membranes with a NaOH solution. The resulting values were compared with those calculated by weighing the membranes before and after the acid uptake. Differences in *DL* of about 10% were found, which are likely related to water adsorption. The doping level is here expressed as the mass of absorbed H_3PO_4 per gram of dry polymer (see Experimental Section), rather than the number of acid molecules per monomer unit, as generally made in the literature. This approach allowed us to obtain normalised doping levels, which is necessary for a proper comparison in case of polymers made from monomers with different weight. Table 1 shows *DL* values obtained for the membranes doped with aqueous solutions of H_3PO_4 at three different concentrations, and namely 30, 50 and 70 wt%. Doping levels in the range 26–99% and 24–77% were found for F_6-oxyPBI and F_6-oxyPBI-2SO_3H membranes, respectively, depending on the acid concentration. As we can see from Table 1, remarkably lower uptakes were measured for the fluoro-PBI systems with respect to meta- or para-PBI, which can be likely correlated to the higher hydrophobic nature of the fluorinated polymers.[19] Furthermore, the sulfonated fluoro-PBI membranes showed even reduced doping at each acid concentration. This phenomenon may be interpreted in terms of interactions between the acid sites of the sulfonic groups and the basic nitrogen of the benzimidazole blocks, that make such N-atoms less available for the dissociation of phosphoric acid. This hypothesis, already discussed in our previous paper,[13] was confirmed by titrating the H_3PO_4 absorbed by both the membranes. Figure S2 (Supporting Information) shows, as an example, the curve obtained by titrating a doped F_6-oxyPBI membrane with NaOH. Two inflection points were identified, at pH = 9.2 and pH = 4.5 respectively, similarly to what obtained by titrating a pure H_3PO_4 solution. The third one was outside the measurement range. The first point corresponds to the titration of free phosphoric acid, whereas the second inflection is referred to the $H_2PO_4^-$ species, coming from the reaction of H_3PO_4 with a base, as reported in the following **Scheme 4**.

From this curve it is possible to quantitatively distinguish the free acid distributed along the chain from the deprotonated species bonded to the basic nitrogen atoms of benzimidazole. This is particularly helpful for the comprehension of the acid complexation mechanism in the membranes, and the identification of

$$H_3PO_4 + OH^- \longrightarrow H_2PO_4^- + H_2O$$

$$H_2PO_4^- + OH^- \longrightarrow HPO_4^{2-} + H_2O$$

Scheme 4. First and second dissociation reactions of H_3PO_4.

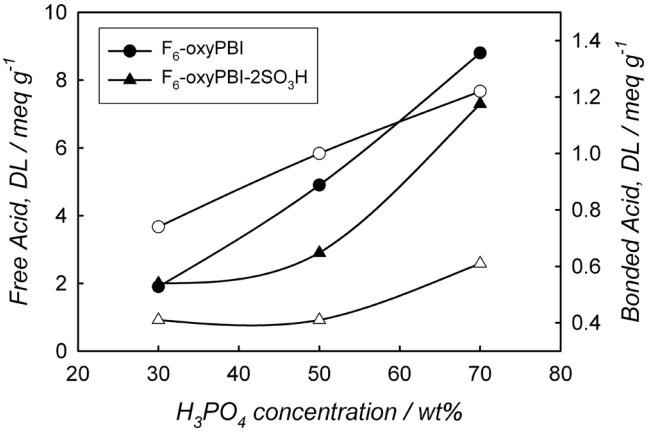

Figure 1. Amounts of the free (full symbols) and bonded (open symbols) acid in the fluoro-PBI based membranes vs. the concentration of the doping H_3PO_4 solution.

complexing sites with higher affinity for the acid.[23,24] **Figure 1** reports the behaviour of the amounts of free H_3PO_4 and bonded $H_2PO_4^-$, derived from the first and second equivalent points respectively, for both the membranes vs. the doping solution concentration. Basically, most of phosphoric acid is present as the free moiety and its amount increases with the H_3PO_4 concentration. The amount of acid bonded to the basic units of benzimidazole is remarkably lower and somehow affected by the monomer structure. In the case of F_6-oxyPBI membranes, the $H_2PO_4^-$ content increased quasi-linearly with the concentration of the doping solution, reaching values about 1.3 meq g^{-1}. In presence of sulfonic groups, a lower number of H_3PO_4 molecules may be bonded to the polymer. The amount of the $H_2PO_4^-$ species, in fact, was about 0.4 meq g^{-1}, and it did not change by varying the acid concentration at least up to 50 wt%. This could substantially mean that the sulfonic units interact with the benzimidazole ring, so thwarting the capability of N-sites to dissociate the phosphoric acid. On the other hand, the quantity of the bonded acid slightly increased in case of more concentrated doping solution, because of balancing massive effects.

The doped F_6-oxyPBI and F_6-oxyPBI-$2SO_3H$ membranes were also investigated from a mechanical point of view, by measuring the elongation and the stress at break at room temperature. This study was performed at two doping levels, in order to address the membrane mechanical durability in presence of phosphoric acid. **Table 2** lists the tensile strength and the elongation at break of the membranes at different doping levels. Variations in the range 16–45 MPa and 3–8%, respectively, were measured depending on the polymer and acid concentration. The doped membranes show worse mechanical properties with respect to the undoped ones, likely due to the plasticising effect of free H_3PO_4, which separates the PBI chains, so reducing the intermolecular forces.[2]

It must be stressed that dramatic decreases of the tensile stress and tensile modulus, as well as enhancements of elongation, were reported in literature. For instance, values of stress at break of meta-PBI changing between 11.2 to 3.6 MPa were obtained by increasing the acid doping level from 6.4 to 11.2, whereas the tensile strength of undoped mPBI was higher than 110 MPa.[19] In contrast, the mechanical properties of F_6-oxyPBI doped membranes did not change with respect to the undoped ones, at least in presence of low doping level (26%). In this case, tensile stress of 45.1 MPa and elongation around 3% were still found. Expected reductions of the tensile stress were obtained for higher doping levels (16.7 MPa at *DL* = 58%). The sulfonated fluoroPBI-based membranes are stiffer due to the lower doping level (see Table 2). The decrease of the mechanical properties of both the F_6-oxyPBI and F_6-oxyPBI-$2SO_3H$ doped membranes seem to be more smaller than those usually reported in literature for the meta- or para-PBI- doped systems. As discussed above, stresses at break around 1–12 MPa and elongations higher than 10% are frequently found, depending on doping level and polymer molecular weight.[2,11,19]

2.4. Proton Conductivity

The proton transport was investigated as a function of both the temperature and the relative humidity. **Figure 2** shows the proton conductivity at 120 °C of F_6-oxyPBI- and F_6-oxyPBI-$2SO_3H$ membranes at two humidity values (30% *R.H.* and 50% *R.H.*) vs. the doping level. The values of PBI_5N are reported for the sake of comparison. As generally observed,[3,5,24] the conductivity increased with *R.H.* This is related to the uptake of water, which enhances the ion mobility by reducing the acid viscosity in the membrane. Inside the two series, as expected, the conductivity increases with the doping level. From Figure 2 it is clear that the F_6-oxyPBI-$2SO_3H$ membrane behaves better than the F_6-oxyPBI one, at least by a factor of two, as soon as the doping level exceeds 30–40%. But the most striking result

Table 2. Some physical and chemical properties of the membranes vs. the doping level (*DL*): mechanical properties, proton conductivity, σ, measured at 120 °C and *R.H.* = 50%, activation energies, E_a, calculated between 70°C and 130°C at *R.H.* = 50%, and the peak power density provided by the corresponding MEAs at 150°C; n.a. = not available.

Membrane	*DL* [%]	Elongation at Break [%]	Stress at Break [MPa]	$\sigma_{120\,°C}$ [mS cm^{-1}]	E_a [kJ mol^{-1}]	Peak power density [mW cm^{-2}]
F_6-oxyPBI	26	3	43	1.8	53.4	n.a.
	58	5	17	11.5	35.5	320
	99	n.a.	n.a.	41.4	n.a.	n.a.
F_6-oxyPBI-$2SO_3H$	24	7	42.8	1.1	40.6	n.a.
	32	8	34	6.2	35.4	360
	77	n.a.	n.a.	49.0	–	n.a.

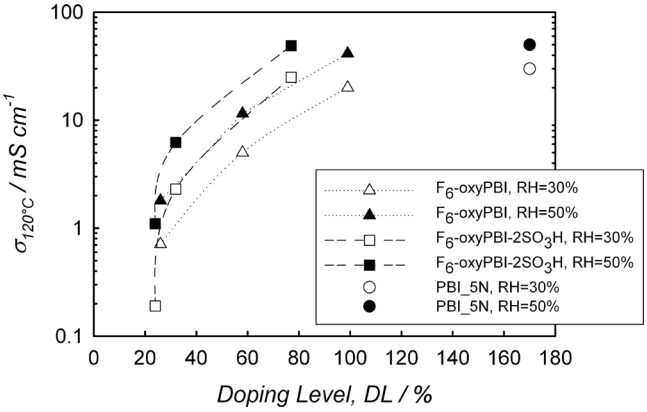

Figure 2. Proton conductivity at 120 °C vs. the doping level at different *R.H.* values

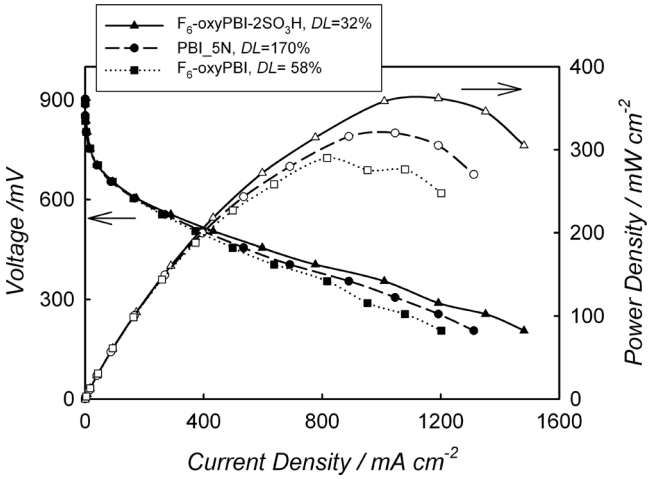

Figure 3. Polarization curves of MEAs based on fluoro- and sulfonated fluoro-oxyPBI membranes at 150 °C and without any external humidification. The data of PBI_5N are shown for the sake of comparison.

of F_6-oxyPBI-2SO_3H, when compared with PBI_5N, is indeed that the same conductivity values (e.g., 40 mS cm^{-1} at 50% *R.H.*) can be obtained with a 55% reduction of the doping level.

A possible criticism, here, is that both the membranes showed conductivity values lower than others reported in the literature.[2] This was expected because these last were prepared with very high doping levels ($N > 8$). We stress again, here, that our target was to find the best compromise between conductivity and reduced H_3PO_4 content (which means better mechanical and chemical stability). Proton conductivity of 41 and 49 mS cm^{-1} were measured at 120 °C and *R.H.* = 50% in case of F_6-oxyPBI and F_6-oxyPBI-2SO_3H membranes (see Table 2), with *DL* of 99% and 77%, respectively. These results are particularly encouraging. In fact, comparable values are reported in the literature in case of meta-or para-PBI membranes, only for higher doping levels (*DL* > 300%)[24] and higher working temperatures (150–200 °C).[2]

The membranes proton transport was also investigated as a function of temperature in the range 70–130 °C at constant relative humidity (*R.H.* = 50%). We obtained good Arrhenius behaviours. The resulting activation energies, E_a, are listed in Table 2. As expected, the activation energies decrease by increasing the doping level. Ma et al.[24] showed that E_a approaches the value obtained for the H_3PO_4 concentrated solution as the doping level increases. This suggests that the proton migration is promoted in presence of an excess of free phosphoric acid, the larger the higher *DL* is.

At low H_3PO_4 concentration (30 wt%), the F_6-oxyPBI-2SO_3H membrane showed lower activation energy than the non-sulfonated one, even if the overall adsorbed acid was comparable. At higher concentrations, in spite of the remarkably lower doping level of the sulfonated membrane, similar E_a values of about 35 kJ mol^{-1} were obtained.

2.5. Fuel Cell Tests and Durability

Figure 3 shows the *I–V* plots of MEAs obtained by using the F_6-oxyPBI and F_6-oxyPBI-2SO_3H membranes, doped with 58 wt% and 32 wt% of H_3PO_4, respectively. The data were collected at 150 °C without gases humidification. The reactants pressure was kept constant at 1 bar. The data are also compared with those obtained on a PBI_5N membrane (*DL* = 170%), which delivered a power density peak of about 310 mW cm^{-2}.[13] The best performances were obtained in the case of the sulfonated membrane, which provided a power density peak of 360 mW cm^{-2}. The F_6-oxyPBI-based MEA provided a power density peak of 290 mW cm^{-2}. OCVs of about 0.9 V and current densities of about 200 mA cm^{-2} at 0.6 V were measured on the cells.

The results reported in Figure 3 are even more significant if we recall that the F_6-oxyPBI-2SO_3H membrane has a doping level (*DL* = 38%) which is about five times lower that that one of PBI_5N (*DL* = 170%). This evidence clearly points out that a higher proton conductivity (see Figure 2) is not the only important aspect in membrane optimization. Rather, the achievement of a compromise among several properties, including transport, mechanical resistance, and chemical compatibility/stability is the true point in developing a performing and durable fuel cell.

The long-term stability of F_6-oxyPBI-2SO_3H MEA was investigated by means of durability tests performed under steady state conditions, at a current load of 0.2 A cm^{-2} and 150 °C without any humidification of the reactant gases. Figure S3 (Supporting Information) reports, as an example, the fuel cell voltage vs. time behaviour of the MEA based on F_6-oxyPBI-2SO_3H membrane obtained after a stabilization period of about 50 h. The cell showed a very stable voltage value of 604 mV over about 800 h, after that a steady decrease to 590 mV was recorded. This corresponds to a membrane degradation rate of about 14 μV h^{-1} during a test period of the order of 1000 h. Higher voltage loss rates during the life test were reported in literature for MEAs based on PBI.[25] Li et al. discussed a dramatic failure in the fuel cell durability tests over short periods (<250 h) with MEAs based on m-PBI and linear hexafluoropropylidene-PBI (F_6PBI) with doping level higher than 8.[19]

The hydrogen crossover rate, which allows determining the permeability of the membrane, is another key parameter in the test protocols for the evaluation of the cell durability.[25–28] The H_2 crossover current corresponds to the oxidation of H_2 molecules at the cathode in presence of the electrocatalyst. This

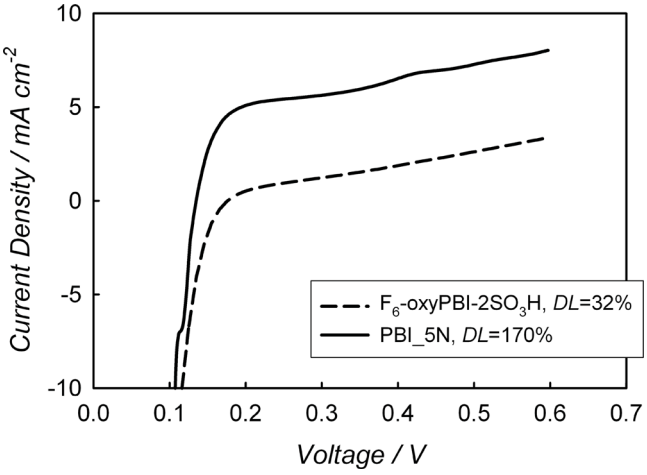

Figure 4. Linear voltammetry sweeps on MEAs based on sulfonated fluoro-oxyPBI and PBI_5N collected for the measurements of the cross-over current density.

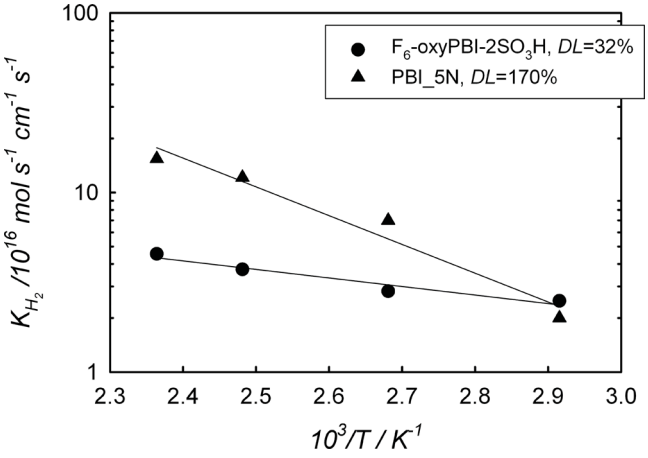

Figure 5. Arrhenius behavior of the hydrogen permeability coefficients for F_6-oxyPBI-2SO_3H and PBI_5N membranes

current reaches a limiting value when a potential of 100–150 mV is applied. If the H_2 crossover dramatically increases, large pinholes or cracks are reasonably formed along the membrane, which compromise the cell life-time. H_2 permeation through F_6-oxyPBI-2SO_3H-based membrane was measured before and after the life test. The curves of the crossover currents are showed in **Figure 4** for the F_6-oxyPBI-2SO_3H and PBI_5N membranes. The H_2 crossover current rapidly increases with the applied voltage, until a plateau is reached around 0.3 V, where the current is limited by the gas permeation kinetics. From the hydrogen crossover current, it is possible to determine the gas permeation coefficient by applying the following equation[29]:

$$k_{H_2} = \frac{i_{H_2}}{nF} \times \frac{l}{p_{H_2}} \quad (1)$$

where i_{H2} is the limiting current obtained from linear voltammetry, I is the membrane thickness and p_{H2} is the hydrogen partial pressure.

Table 3 reports the hydrogen crossover currents, i_{H2}, for MEAs based on the fluoro-sulfonated PBI and PBI_5N membranes, after the life-tests, measured at p_{H2} of 1 bar in the temperature range of 70–150 °C. The F_6-oxyPBI-2SO_3H membrane has a hydrogen permeability much lower than that of the PBI_5N one. The gas permeation of the two investigated MEAs was also determined after the durability test at 150 °C.

Table 3. Hydrogen crossover current through the investigated doped membranes; p_{H2}: 1 bar; membrane thickness: i) F-oxyPBI-2SO_3H: 80 µm; ii) PBI_5N: 90 µm.

	i_{H2} [mA cm^{-2}]	
T [°C]	F_6-oxyPBI-2SO_3H 32% H_3PO_4	PBI_5N 170% H_3PO_4
70	0.6	0.7
100	0.7	1.5
130	0.9	2.6
150	1.1	3.3

Both the membranes showed a i_{H2} change of roughly a factor of 2 after 1000 h under a current load of 200 mA cm^{-2}. Dramatic enhancements in the hydrogen permeability (up to ten times) were reported in literature at temperature higher that 160 °C over test period of at least 800 h[25,30] The excellent performances of the F_6-oxyPBI-2SO_3H membranes are likely due to the higher stiffness and mechanical robustness of this new polymer with respect to other linear PBIs (e.g., meta- or para-PBI), which hinders common degradation phenomena, such as the progressive thinning and the pinhole/crack formation.

As already stated, the crossover current allows estimating the H_2 permeability coefficient, k, in terms of Equation (2). **Figure 5** shows the behavior of k as a function of temperature for both the fuel cells at 150 °C and p_{H2} = 1 bar. The membrane thickness was 80 µm for F_6-oxyPBI-2SO_3H- and 90 µm for PBI-5N, respectively. As expected, a linear trend was observed in both cases. Higher coefficients, k, were obtained for the PBI_5N membrane. In case of the fluoro-sulfonated membrane, k between 2.49 and 4.55 × 10^{-16} mol cm^{-1} s^{-1} Pa^{-1} were obtained in the temperature range 70–150 °C. These values are quite comparable to those determined for wet membranes of Nafion 112 at 80 °C (≈5 × 10^{-16} mol cm^{-1} s^{-1} Pa^{-1}).[29] Higher permeability was reported by Li et al. for PBI membranes with higher *DL*s, namely 1.20–4.00 × 10^{-15} mol cm^{-1} s^{-1} Pa^{-1}, depending on both temperature and H_3PO_4 doping levels.[31]

The activation energies for hydrogen permeation were estimated to be 3.9 kJ mol^{-1} for the F_6-oxyPBI-2SO_3H membrane and 13.3 kJ mol^{-1} for the PBI_5N one. Higher $E_{a,H2}$ of about 21 kJ mol^{-1} was calculated for Nafion membranes in the temperature range between 25 and 80 °C under fuel cells conditions.[29] Finally, no OCV decreases were observed during the fuel cells operation, which further confirmed the absence of significant degradation phenomena, at least over 1000 h life-test.

The degradation tests were supported by electrochemical impedance spectroscopy experiments, performed on MEAs at different current loadings, before and after the life tests. In each case, the impedance spectra showed only one depressed semicircle, in agreement with what already reported for such systems.[32] Figure S4a (Supporting Information) shows, as an example, the Nyquist plots obtained for the MEA based

on F_6-oxyPBI-2SO_3H membrane at different current loadings. The spectra may be fitted with equivalent models shown in Figure S4b (Supporting Information; see ref. [33,34]). This will be the subject of future work.

3. Conclusions

Two novel PBIs, namely hexafluoropropylidene oxyPBI and bisulfonated hexafluoropropylidene oxyPBI, were successfully synthesized with high molecular weight and reproducible polysulfonation degree. The polymers were activated by H_3PO_4 solutions at different concentrations, and doping levels ranging between 24 and 99 wt% were obtained. The doped membranes showed good mechanical properties. The presence of the protogenic groups affected the maximum acid uptake, as well as the proton conductivity of the membranes. In spite of doping level and proton conductivity lower than those of standard PBI membranes, very promising fuel cells performances were obtained for the MEAs based on F_6-oxyPBI-2SO_3H membrane with *DL* = 32%. In particular, *OCV* values higher than 0.9 V and power densities in excess of 360 mW cm^{-2} were obtained at 150°C without any external gas humidification in H_2/air configuration. Contrary to the meta-PBI or F_6-PBI, which showed a dramatic decay in a relatively short test period, MEA based on the fluoro-sulfonated PBI did not undergo degradation during 800–1000 h. This membrane also showed a very low H_2 permeability even after the life test, and this further confirms the absence of degradation phenomena, such as thinning or pinhole/cracks formation. All these encouraging results, in terms of synthesis friendliness and cost, chemical, mechanical and electrochemical stability, show that it is possible to obtain performing and durable membranes for HT-PEMFCs even in presence of reduced acid doping level. The proper design of new materials by means of the introduction of suitable functionalities seems to offer promising opportunities.

4. Experimental Section

Polymer Synthesis: F_6-oxyPBI and F_6-oxyPBI-2SO_3H were obtained starting from properly-designed fluorinated monomers. In case of sulfonated polymers, the polysulfonation was carried out before the polymerization step, as already discussed in our recent paper.[13] All the chemicals were reagent grade and were used as received, unless otherwise mentioned.

Synthesis of Monomers: Two BI-based monomers (F_6-oxyBI and F_6-oxyBI-2SO_3H) were obtained in very high yields and purity through a two-step reaction between fluorinated dialdehyde and benzoaminic acid, starting from cheap commercial chemicals, as sketched in Scheme 1,2a,b.

Synthesis of Fluorinated Dialdehyde I: The dialdehyde was prepared by means of MAOS from Bisphenol AF, 4-fluorobenzaldehyde, potassium bicarbonate, dissolved in dimethylacetamide (DMAc) into a two-necks round bottom flask equipped with a condenser under a N_2 blanket. The oven maximum power was set at 400 W. The mixture was heated at 165 °C for 90 min. After cooling, it was poured into water, and the resulting precipitate was filtered and finally washed with 5 mL of isopropyl ether. The product yield was 80%.

^{1}H NMR (300 MHz; DMSO): δ (ppm) 9.96 (s, 2H), 7.97(d,4H), 7,45(d,4H), 7.24 (m,8H). ^{13}C NMR (300 MHz; DMSO): δ (ppm) 191.5, 161.0, 156.0, 132.0, 131.8, 129.7, 124.1 (q, J = 285 Hz), 119.4, 118.7, 118.2, 63.3 (sept, J = 24.8 Hz).

Synthesis of Fluorinated Monomer F_6-oxyBI (II): The fluorinated dialdehyde I was suspended in a 40% solution of sodium metabisulfite in water. The mixture was stirred for 2 h at room temperature, then a suspension of of 3,4-diaminobenzoic acid in EtOH was added. The solution was heated for 3 h and then cooled at room temperature. The resulting product was isolated by filtration and washed with water to eliminate residual traces of bisulfite adduct. The obtained diacid (F_6-oxyBI, II) was finally recrystallized from a dimethylsulfoxide (DMSO)/water mixture. The product yield was 95%.

IR ν (cm^{-1}): da 3400 a 2400 (OH); 1699 (C = O). ^{1}H NMR (300 MHz; DMSO): δ (ppm) 8.36 (d, 4H), 8.24 (s, 2H), 7.96 (d, 2H), 7.76 (d, 2H), 7.45 (d, 4H), 7.33 (d, 4H), 7.24 (d, 4H). ^{13}C NMR (300 MHz; DMSO): δ (ppm) 167.26, 158.62, 156.48, 151.70, 139.09, 135.88, 131.77, 129.75, 127.57, 126.11, 125.76, 124.88, 122.25, 119.48, 118.92, 116.16, 114.25, 63.46. M.P.: >250 °C.

Synthesis of Fluorosulfonated Monomer (F_6-oxyBI-2SO_3H, III): The diacid II was suspended in chlorosulfonic acid. The mixture was stirred at room temperature for 2 hours to obtain a selective disulfonation (III). The solution was cooled into ice and the resulting sulfonated monomer was isolated by filtration. The solid was washed with water till to the neutrality. Even in this case, the monomer yield was 95%.

IR ν (cm^{-1}): da 3400 a 2400 (OH); 1699 (C = O). ^{1}H NMR (300 MHz; DMSO): δ (ppm) 7.99 (s, 1H), 7.92 (m, 4H), 7.57 (d, 2H), 7.37 (d, 4H), 7.06 (d, 4H), 6.80 (d, 2H). ^{13}C NMR (300 MHz; DMSO): δ (ppm) 176.3, 156.46, 154.52, 144.65, 142.02, 134.54, 132.73, 130.09, 128.99, 128.29, 127.87, 126.92, 125.50, 122.56, 121.68, 119.76, 119.04, 116.53, 114.24, 63,62. ^{13}C NMR DEPT (300MHz; DMSO): δ (ppm) 134.5, 130.1, 128.3, 122.6, 119.8, 119.0, 116.5, 114.2. M.P.: >250 °C

Polymerization: The polymers, P-II and P-III (see Scheme 3), were synthesized by the polycondensation approach reported in ref. [13]. Proper amounts of the corresponding monomer, II and III respectively, were mixed with 3,3′-diaminobenzidine and PPA (polyphosphoric acid) into a two necked, round-bottom flask equipped with mechanical stirrer and under N_2 inert atmosphere. The mixture was heated at 200 °C for 7 h. The resulting black and viscous solutions were poured in water obtaining tough filaments. The polymers were subsequently washed with a solution of NaOH (10 wt% in water) and finally dried.

Membrane Preparation: Proper amounts of polymers were dissolved in a mixture of dimethylacetamide (DMA)/sec-butylamine/water at 180 °C in a sealed vessel under MAOS. Microwave-assisted synthesis were performed in a MicroSYNTH oven (Milestone), equipped with an optical fibre temperature probe and power control. The oven frequency is 2.45 GHz. The solution was poured in a Petri dish and heated through subsequent drying steps, at 50 °C for 24 h and 120 °C for 10 h, respectively, in order to totally remove the solvents. The thickness of the resulting films was about 80 μm. The membranes were then washed in hot water, immersed in three different phosphoric acid concentrations, namely 30, 50, 70 wt%, for at least 48 h up to reach the equilibrium, and finally dried at 110 °C overnight. The doping level, *DL* (%), was calculated as membrane weight increase, calculated by the following formula

$$DL_{PA} = \frac{W_{PA}}{W_{dry\text{-}PBI}}\% \quad (2)$$

where $W_{dry\text{-}PBI}$ is the weight of the membrane before the acid uptake and W_{PA} is the mass of absorbed H_3PO_4. The amount of up-taken acid was determined by two approaches: i) by weighing the membrane before and after the immersion in acid; and ii) by titration of the membrane in a NaOH solution (0.1 M) using a pH-meter for a continuous monitoring. The agreement between the two techniques is better than 10%. The data are reported in Table 1.

Characterizations: High-resolution NMR spectra of the monomers were collected with a Bruker 300 MHz spectrometer, by using dimethylsulfoxide (DMSO-d_6) as the solvent. IR spectra were obtained by means of a FT-IR spectrometer (Perkin Elmer), placing the samples into a NaCl cell. ESI-MS spectra of the monomers were obtained by means of a Thermo Scientific LTQ-XL mass spectrometer, by dissolving the sample in a mixture

DMSO:MeOH 1:10. Polymer Intrinsic Viscosity (*I.V.*) was determined with an Ubbelohde viscosimeter at 50 °C in sulfuric acid. TGA scans were recorded at 5 °C min^{-1} under nitrogen flow with a 2950 TGA microbalance (TA Instruments). The proton conductivity was measured by means of both DC and AC techniques fixing the membrane to a four-points BekkTech conductivity cell, connected to the test stand BekkTech 411 for the humidity and temperature control. In case of AC measurements, the impedance spectroscopy was carried out by using a frequency response analyser (FRA Solartron 1255), connected to an electrochemical interface (Solartron 1287), over the frequency range 1 Hz-1 MHz at a voltage of 100 mV. The impedance scans were performed at 120 °C ranging from 1.5 to 70% R.H. with a cell back-pressure of 2.0 bar. The films were allowed to equilibrate 1 h at each moisture level before of the measurements. The impedance spectra were fitted with the Z-View 3.0 software (Scribner Associates, Inc.). The membrane electrode assemblies (MEAs) were prepared by hot pressing two gas diffusion electrodes (GDE HT-ELAT, ETek) at 130 °C and 1 ton for 10 min. The Pt loading was 0.5 mg cm^{-2} at both the electrodes. The cell active area was 5 cm^2. The electrochemical measurements were performed at 150°C with a BT-552 Membrane Conductivity and Single Cell Fuel Cell Test System (BekkTech LLC) in the temperature range 110–150 °C. The cell was operated at ambient pressure without external humidification of the feed gas steams. In some cases an overpressure was imposed to the cell. The H_2 and air flow rates were 70 sccm and 300 sccm, respectively. The durability tests were performed at a constant current loading of 200 mA cm^{-2} for 1000 h.

Hydrogen crossover measurements were carried out in the temperature range 70–150 °C by means of potentiodynamic scans between 0 and 0.7 V. The cathode gas flow was switched from air to nitrogen, with a flow rate of 400 sccm at 1 bar, whereas the anode hydrogen flow was set at 200 sccm at the same pressure. The anode was taken as both counter and reference electrode, whereas the cathode served as the working one. A potentiostatic assessment at the voltage plateau (0.3 V) was finally performed to measure the current through the fuel cell for 15 min at each temperature.

Acknowledgements

This project was financed by Italian Ministry of University and Research (MIUR) (PRIN 2010, 2010CYTWAW). The authors are also thankful to Dr. S. Lanati and Dr. N. Santini (ITP SpA) for the mechanical tests.

Received: December 19, 2013
Revised: March 7, 2014
Published online:

[1] DOE Fuel Cells Technical Plan, Hydrogen and Fuel Cells Programs (2012), www1.eere.energy.gov/hydrogenandfuelcells/mypp/pdfs/fuel_cells.pdf (accessed February 2014).
[2] Q. Li, J. O. Jensen, R. F. Savinell, N. J. Bjerrum, *Prog. Polym. Sci.* **2009**, *34*, 449.
[3] E. Quartarone, P. Mustarelli, *Energy Environ. Sci.* **2012**, *5*, 6436.
[4] H. Zhang, P. K. Shen, *Chem. Rev.* **2012**, *112*, 2780.
[5] A. Carollo, E. Quartarone, C. Tomasi, P. Mustarelli, F. Belotti, A. Magistris, F. Maestroni, M. Parachini, L. Garlaschelli, P. P. Righetti, *J. Power Sources* **2006**, *160*, 175.
[6] S. Angioni, P. P. Righetti, E. Quartarone, E. Dilena, P. Mustarelli, A. Magistris, *Int. J. Hydrogen Energy* **2011**, *36*, 7174.
[7] J. Li, Y. Zhao, W. Lu, Z. Shao, B. Yi, *ChemSusChem.* **2012**, *5*, 896.
[8] D. C. Villa, S. Angioni, E. Quartarone, P. P. Righetti, P. Mustarelli, *Fuel Cells* **2013**, *13*, 98.
[9] P. Mustarelli, E. Quartarone, S. Grandi, A. Carollo, A. Magistris, *Adv. Mater.* **2008**, *20*, 1339.
[10] E. Quartarone, P. Mustarelli, A. Carollo, S. Grandi, A. Magistris, C. Gerbaldi, *Fuel Cells* **2009**, *9*, 231.
[11] E. Quartarone, A. Magistris, P. Mustarelli, S. Grandi, A. Carollo, G. Z. Zukowska, J. E. Garbaeczyk, J. L. Nowinski, C. Gerbaldi, S. Bodoardo, *Fuel Cells* **2009**, *9*, 349.
[12] J. Yang, D. Aili, Q. Li, Y. Xu, P. Liu, Q. Che, J. O. Jensen, N. J. Bjerrum, R. He, *Polym. Chem.* **2013**, *4*, 4768.
[13] S. Angioni, D. C. Villa, S. Dal Barco, E. Quartarone, P. Mustarelli, C. Tomasi, P. P. Righetti, *J. Mater. Chem. A* **2014**, *2*, 663.
[14] S.-W. Chuang, S. L.-C. Hsu, *J. Polym. Sci. A* **2006**, *44*, 4508.
[15] S.-W. Chuang, S. L.-C. Hsu, Y.-H. Liu, *J. Membr. Sci.* **2007**, *305*, 353.
[16] S. C. Kumbharkar, Md. N. Islam, R. A. Potrekar, U. K. Kharul, *Polymer* **2009**, *50*, 1403.
[17] J. T.-W. Wang, S. L.-C. Hsu, *Electrochimica Acta* **2011**, *56*, 2842.
[18] G. Qjan, B. C. Benicewicz, *J. Polym. Sci. A* **2009**, *47*, 4064.
[19] J. Yang, Q. Li, L. N. Cleemann, J. O. Jensen, C. Pan, N. J. Bjerrum, R. He, *Adv. Energy Mater.* **2013**, *3*, 622.
[20] J. A. Mader, B. C. Benicewicz, *Fuel Cells* **2011**, *11*, 212.
[21] H. Dai, H. Zhang, H. Zhong, H. Jin, X. Li, S. Xiao, Z. Mai, *Fuel Cells* **2010**, *10*, 754.
[22] J. H. Liao, Q. F. Li, H. C. Rudbeck, J. O. Jensen, A. Chromik, N. J. Bjerrum, J. Kerres, W. Xing, *Fuel Cells* **2011**, *11*, 745.
[23] R. He, Q. Li, J. O. Jensen, N. J. Bjerrum, *J. Polym. Sci. A* **2007**, *45*, 2989.
[24] Y.-L. Ma, J. S. Wainright, M. H. Litt, R. F. Savinell, *J. Electrochem. Soc.* **2004**, *151*, A8.
[25] A. D. Modestov, M. R. Tarasevich, V. Ya. Filimonov, N. M. Zagudaeva, *Electrochimica Acta* **2009**, *54*, 7121.
[26] K. C. Neyerlin, A. Singh, D. Chu, *J. Power Sources* **2008**, *176*, 112.
[27] Y. Oono, A. Sounai, M. Hori, *J. Power Sources* **2013**, *241*, 87.
[28] Y. Oono, A. Sounai, M. Hori, *J. Power Sources* **2012**, *210*, 366.
[29] S. S. Kocha, J. D. Yang, J. S. Yi, *Aiche J.* **2006**, *52*, 1916.
[30] S. Galbiati, A. Baricci, A. Casalegno, R. Marchesi, *Int. J. Hydrogen Energy* **2013**, *38*, 6469.
[31] R. He, Q. Li, A. Bach, J. O. Jensen, N. J. Bjerrum, *J. Membr. Sci.* **2006**, *277*, 38.
[32] V. Kurdakova, E. Quartarone, P. Mustarelli, A. Magistris, E. Caponetti, M. Saladino, *J. Power Sources* **2010**, *195*, 7765.
[33] J. Zhang, Y. Tang, C. Song, J. Zhang, *J. Power Sources* **2007**, *172*, 163.
[34] J. L. Jespersen, E. Schaltz, S. K. Kaer, *J. Power Sources* **2009**, *191*, 289.